

NUMERICAL VARIATIONAL ANALYSIS FORMULATED UNDER THE CONSTRAINTS AS DETERMINED BY LONGWAVE EQUATIONS AND A LOW-PASS FILTER

YOSHIKAZU SASAKI

The University of Oklahoma, Norman, Okla.

ABSTRACT

The "timewise localized" variational formalism of the numerical variational analysis method is used (1) to filter and suppress unnecessary high-frequency noises contained in initial and forecast fields and (2) to obtain dynamically sound initial values in the areas lacking data. A set of nonlinear longwave equations and a low-pass filter minimizing local changes are used in this paper as dynamical constraints. Also proposed in this study is a technique to assure the convergence of a numerical solution of the nonlinear Euler equations by an iterative process.

Three applications of the method are presented. The first two examples demonstrate that the initial guess in the iterative process influences significantly the speed of convergence. The last example is an application to the 500-mb analysis of hurricane Dora, 1964, and demonstrates a reasonable analysis in the data-sparse area where the hurricane was located at 1200 GMT on Sept. 8, 1964.

1. INTRODUCTION

The study of objective analysis techniques has been one of the most important areas of research in meteorology in recent years. These methods attempt to construct fields of optimized values of meteorological variables at specified grid points based on irregularly distributed observed data. These objectively analyzed values may then be used as initial data for a numerical prediction of the meteorological fields. The objective analysis methods currently used on a routine basis follow these steps (Cressman 1959, Gandin 1965): transmitting observed data from meteorological stations to the computer, decoding the data for the objective analysis, interpolating the values from the station values at the prespecified grid points, matching the interpolated values to prespecified statistical and/or diagnostic conditions, and eliminating data that have apparent errors and then preparing them for use in the numerical prediction.

Considerable effort in the initial development of objective analysis has led to its successful routine operation on a daily basis. However, some improvements can be made on the interpolation and matching stages because the fields analyzed by the conventional objective analysis methods are not necessarily consistent with the conditions implied in a numerical prediction model. This inconsistency becomes more apparent when primitive equations are used for prediction; it results in the generation of undesirable high-frequency noises in the forecasted fields. If the data are used directly, high-frequency modes, for example, a short-period oscillation of motion, will be generated due to the possibility of generating high frequencies in prognostic schemes in the course of time integration of the prognostic equations. The inconsistency arises primarily from sparsity and inaccuracy of data, irregularity of data distribution, and an unsatisfactory initialization process.

As technology in the area of numerical weather prediction has progressed over the last two decades, the prediction models to promote higher accuracy of prediction have been including more physical waves that were filtered out in the earlier prediction models, namely, the quasi-geostrophic models. The primitive equation models used in recent years contain internal and external gravity waves that in the quasi-geostrophic models are filtered as "meteorological noise." Along with this trend in the prediction models, proper determination of the initial conditions has been recognized as important to suppressing the unnecessary part of the physical waves. Phillips (1960) suggested that, theoretically, the initial condition of wind and pressure fields is determined by the summation of geostrophically balanced components and the divergent component calculated from the ω equation. This suggestion is in agreement with the numerical result obtained by Hinkelmann (1959). Hinkelmann demonstrated, using his five-layer primitive equation model, that the high-frequency oscillations of the period of about 6–8 hr in the predicted ω field were suppressed when the initial divergent part of the wind was given from the ω equation. High-frequency oscillation will be filtered out, generally speaking, if the initial fields are so constructed that the time derivatives of divergence vanish in the initial field: $\partial^n q / \partial t^n = 0$ where q is divergence and $n=1, 2, 3, \dots$. The balance equation (Charney 1955, Bolin 1955), which has been widely used to obtain the initial stream function, is a diagnostic equation derived from the primitive equations for a two-dimensional incompressible flow under the above condition for $n=1$. The condition for both $n=1$ and 2 was used by Miyakoda and Moyer (1968) and Nitta and Hovermale (1969). Instead of deriving diagnostic equations, they directly used the primitive equations to adjust the initial fields by the iterative process of integrating forward and backward until the solution satisfies the condition,

A different approach to the initial field analysis has been taken by the author who introduced the variational method to obtain dynamically sound initial fields. He showed theoretically that quasi-geostrophically balanced fields or always divergent free fields could be obtained as a solution to the Euler or Euler-Lagrange equations (Sasaki 1958). Later, a direct approach to filtering high-frequency oscillations was proposed by the author (Sasaki 1969*a*, 1969*b*, 1970*a*, 1970*b*). The method was explained by two simple examples, the linear advection equation and the linear diffusion equation used as prognostic equations. The basic idea is to use the above condition as a low-pass filter in a broader sense by taking q , not limited to divergence, as a meteorological parameter to be filtered. Characteristics of filtering high-frequency modes by the method are favorable because of the monotonic shape of the low-pass filter. Continuing study has been done by the author in this article and the author with Lewis (1970) by considering various nonlinear systems of prognostic equations as dynamical constraints in numerical variational objective analysis. This article describes the method applied to a case where longwave equations are used with quasi-steady state conditions as a dynamical constraint. Also, a technique to obtain a converging solution for simultaneous nonlinear Euler equations is proposed in this article. Finally, application of the method to the data of hurricane Dora, 1964, is discussed to show whether or not the method generates reasonable fields in the data-sparse areas.

2. DYNAMICAL CONSTRAINTS

Two-dimensional barotropic motion in an inviscid, incompressible, hydrostatic fluid is considered as a dynamical constraint. The fluid has a free surface in a middle latitude on the earth. Such motion represents longwaves or shallow water waves and is described by the following set of equations:

$$\frac{\partial u}{\partial t} + u \frac{\partial u}{\partial x} + v \frac{\partial u}{\partial y} - fv + \frac{\partial \varphi}{\partial x} = 0, \tag{1}$$

$$\frac{\partial v}{\partial t} + u \frac{\partial v}{\partial x} + v \frac{\partial v}{\partial y} + fu + \frac{\partial \varphi}{\partial y} = 0, \tag{2}$$

and

$$\frac{\partial \varphi}{\partial t} + \frac{\partial}{\partial x}(\varphi u) + \frac{\partial}{\partial y}(\varphi v) = 0 \tag{3}$$

where u and v are the horizontal velocity components, respectively, in the x (east) and y (north) direction on a Cartesian coordinate system; φ is the geopotential defined as gh , g and h being the acceleration of gravity and the height of the free surface, respectively; and f is the Coriolis parameter, assumed constant in this study.

If fluctuation of the height of the free surface is small compared with the constant mean height H , the nonlinear terms φu and φv are approximated by Φu and Φv where Φ is gH and constant. In this case, eq (3) is written

as

$$\frac{\partial \varphi}{\partial t} + \Phi \left(\frac{\partial u}{\partial x} + \frac{\partial v}{\partial y} \right) = 0. \tag{3'}$$

To filter out high-frequency components of disturbances, one uses the following set of conditions:

$$\frac{\partial u}{\partial t} = 0, \quad \frac{\partial v}{\partial t} = 0, \quad \text{and} \quad \frac{\partial \varphi}{\partial t} = 0. \tag{4}$$

Each of these conditions represents near-steadiness of the corresponding field. The essential characteristics of this type of filter were discussed in the author's previous paper (1969*b*). The condition of steadiness of the φ field can be applied for eq (3) instead of eq (3'). The set of eq (1), (2), and (3) satisfies the conservation of the total energy:

$$\frac{\partial}{\partial t} \int_{\Omega} \frac{\varphi}{2} (u^2 + v^2 + \varphi) d\omega = 0 \tag{5}$$

where Ω is the domain of consideration and $d\omega$ is the element of domain, while the set of eq (1), (2), and (3') does not. The conservation requires the proper boundary condition that does not allow the net total energy flux to pass through the entire boundary:

$$\oint_S v_n \frac{\varphi}{2} (u^2 + v^2 + \varphi) ds = 0 \tag{6}$$

where S is the entire boundary of the domain Ω , ds is the segment of the boundary, and v_n is the wind component normal to the boundary. The dynamical constraints employed in the present study will be (1), (2), (3), and (4).

3. GRID SYSTEM

The grid system used in this study is shown in figure 1. The averaged quantities are denoted by $\langle u \rangle$, $\langle v \rangle$, $\langle \varphi \rangle_x$ and $\langle \varphi \rangle_y$. The variables u , $\langle v \rangle$, and $\langle \varphi \rangle_x$ are assigned on the same grid points; and v , $\langle u \rangle$ and $\langle \varphi \rangle_y$ are on the set of other grid points. The average $\langle u \rangle$ is calculated by taking the arithmetic averages of the four nearest u values around the grid point where $\langle u \rangle$ is assigned. The average $\langle v \rangle$ is determined similarly. The average $\langle \varphi \rangle_x$ is an arithmetic average of the two nearest φ on the x axis at the grid point of $\langle \varphi \rangle_x$.

These definitions are expressed using an arbitrary variable ξ assigned on the grid points as

$$\langle \xi \rangle = \frac{\xi_{i,j} + \xi_{i+1,j} + \xi_{i,j+1} + \xi_{i+1,j+1}}{4},$$

$$\langle \xi \rangle_x = \frac{\xi_{i,j} + \xi_{i+1,j}}{2},$$

and

$$\langle \xi \rangle_y = \frac{\xi_{i,j} + \xi_{i,j+1}}{2} \tag{7}$$

where the subscripts i and j are integers defined in such a

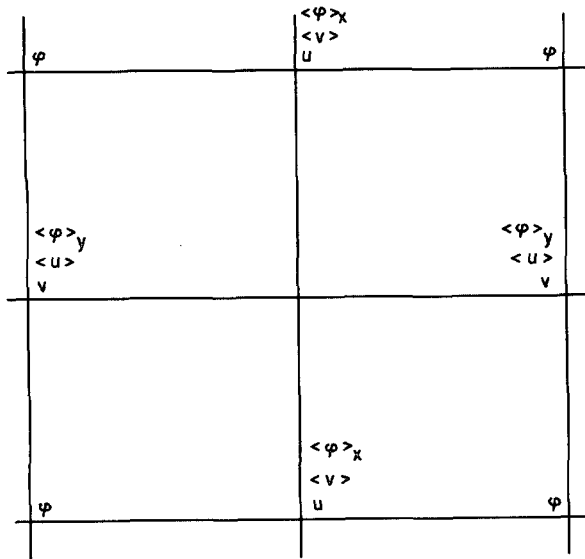


FIGURE 1.—Grid system.

way that i or j increases respectively as x increases or y decreases.

The finite-difference operators, $\nabla_t, \nabla_x, \nabla_y, \bar{\nabla}_x, \bar{\nabla}_y$, and ∇^2 , which appear in subsequent sections, are defined as

$$\nabla_t \xi = \frac{1}{2\Delta t} (\xi_{n+1} - \xi_{n-1}),$$

$$\nabla_x \xi = \frac{1}{2\Delta x} (\xi_{i+1,j} - \xi_{i,j}),$$

$$\nabla_y \xi = \frac{1}{2\Delta y} (\xi_{i,j} - \xi_{i,j+1}),$$

$$\bar{\nabla}_x \xi = \frac{1}{4\Delta x} (\xi_{i+1,j} - \xi_{i-1,j}),$$

$$\bar{\nabla}_y \xi = \frac{1}{4\Delta y} (\xi_{i,j-1} - \xi_{i,j+1}),$$

and

$$\nabla^2 \xi_{i,j} = \frac{1}{\Delta x^2} (\xi_{i+1,j} + \xi_{i-1,j} - 2\xi_{i,j}) + \frac{1}{\Delta y^2} (\xi_{i,j-1} + \xi_{i,j+1} - 2\xi_{i,j})$$

where Δx and Δy are the grid size in the x and y directions, respectively. The subscript n represents the n th time level with the time increment being Δt . The grid system is assumed as the same at each time level.

The operators $\nabla_x, \nabla_y, \bar{\nabla}_x, \bar{\nabla}_y, \langle \rangle, \langle \rangle_x$, and $\langle \rangle_y$ are used under rules

$$\Sigma \eta \langle \xi \rangle = \Sigma \langle \eta \rangle \xi \tag{9}$$

and

$$\Sigma \eta \nabla \xi = -\Sigma \xi \nabla \eta \tag{10}$$

where η is also an arbitrary variable, function, or functional; ∇ represents also $\nabla_x, \nabla_y, \bar{\nabla}_x$, or $\bar{\nabla}_y$; $\langle \rangle$ may be $\langle \rangle_x$ or $\langle \rangle_y$; and Σ is a summation over the entire grid points. Proof of eq (9) is given in appendix 1 and the proof of eq (10) is given in the author's article (1969b). The rules (9) and (10), respectively, state that the operator $\langle \rangle$

is commutative and that the operation ∇ is not commutative. These rules can be applied repeatedly.

4. VARIATIONAL FORMALISM

Based on the principle of variational optimality employed in the author's previous studies (1958, 1969a, 1969b), a variational formalism is made:

$$\begin{aligned} \delta J = \delta \sum_{i,j} \{ & \tilde{\alpha}(\phi - \tilde{\phi})^2 + \tilde{\gamma}(u - \tilde{u})^2 + \tilde{\gamma}(v - \tilde{v})^2 \\ & + \alpha_t(\nabla_t \phi)^2 + \gamma_t(\nabla_t u)^2 + \gamma_t(\nabla_t v)^2 \\ & + \alpha[(\nabla_x \phi)^2 + (\nabla_y \phi)^2] + \gamma_u[(\nabla_x u)^2 + (\nabla_y u)^2] \\ & + \gamma_v[(\nabla_x v)^2 + (\nabla_y v)^2] \} = 0. \end{aligned} \tag{11}$$

The $\tilde{\alpha}$ and $\tilde{\gamma}$ terms represent the natural universal requirement of minimizing differences between the observed and analyzed values. If a pressure height observation is not available at a grid point, $\tilde{\alpha}$ may be taken to be zero. However, for assuring convergence of solution of the iterative process, $\tilde{\phi}$ at such a grid point is taken as an average of the surrounding observations, and $\tilde{\alpha}$ is kept the same although a small value is desirable for $\tilde{\alpha}$. The same technique is used for wind. This technique is discussed also in the author's article (1970b). The α_t and γ_t terms are added to satisfy the condition (4) of quasi-steadiness. The α_t, γ_u , and γ_v terms are introduced to solve the Euler or Euler-Lagrange equations of eq (11) as a boundary value problem (Sasaki 1970a) and to assure convergence of the solution as will be discussed in section 5. The α_t, γ_u , and γ_v terms are rather optional in this formalism and should be kept minimal.

The dynamical constraints represented by eq (1), (2), and (3) are written in a finite-difference form using the previously described grid system and operators as

$$\nabla_t \phi = -\nabla_x \langle \phi \rangle u - \nabla_y \langle \phi \rangle v, \tag{12}$$

$$\nabla_t u = f \langle v \rangle - \nabla_x \phi - (u \bar{\nabla}_x u + v \bar{\nabla}_y u), \tag{13}$$

and

$$\nabla_t v = -f \langle u \rangle - \nabla_x \phi - (\langle u \rangle \bar{\nabla}_x v + v \bar{\nabla}_y v). \tag{14}$$

After substitution of eq (12), (13), and (14) into the terms of $\nabla_t u, \nabla_t v$, and $\nabla_t \phi$ in eq (11), the calculus of variation, represented by δ , is now performed on the sum with respect to u, v , and ϕ . The weights $\tilde{\alpha}, \tilde{\gamma}, \alpha_t$, and γ_t remain unvaried. This variation led to the three Euler-Lagrange equations (Courant and Hilbert 1953). These equations are

$$\tilde{\alpha}(\phi - \tilde{\phi}) + \gamma_t [\nabla_x \nabla_t u + \nabla_y \nabla_t v] + \alpha_t [(\nabla_x \nabla_t \phi)_x + (\nabla_y \nabla_t \phi)_y] - \alpha \nabla^2 \phi = 0, \tag{15}$$

$$\begin{aligned} \tilde{\gamma}(u - \tilde{u}) + \alpha_t \langle \phi \rangle_x \nabla_x \nabla_t \phi - \gamma_t f \langle v \rangle + \gamma_t [\bar{\nabla}_x (u \nabla_t u) + \bar{\nabla}_y (\langle v \rangle \nabla_t u) \\ - \nabla_t u \bar{\nabla}_x u - \langle \nabla_t v \bar{\nabla}_x v \rangle] - \gamma_u \nabla^2 u = 0, \end{aligned} \tag{16}$$

and

$$\begin{aligned} \tilde{\gamma}(v - \tilde{v}) + \alpha_i \langle \varphi \rangle_{\nu} \nabla_{\nu} \nabla_i \varphi + \gamma_i f \langle \nabla_i v \rangle + \gamma_i [\bar{\nabla}_x \langle (u) \nabla_i v \rangle + \bar{\nabla}_{\nu} (v \nabla_{\nu} v) \\ - \langle \nabla_i u \bar{\nabla}_{\nu} u \rangle - \nabla_i v \bar{\nabla}_{\nu} v] - \gamma_v \nabla^2 v = 0. \end{aligned} \quad (17)$$

The derivation is given in appendix 2.

5. ITERATIVE METHOD

Solutions of φ , u , and v of the Euler eq (15), (16), and (17) may be obtained by an iterative method. Let a guess field be written as $\varphi^{(\nu)}$, $u^{(\nu)}$, and $v^{(\nu)}$. Substitution of them into the Euler equations will result in residuals on the right-hand sides of the equations:

$$\begin{aligned} \tilde{\alpha}(\varphi^{(\nu)} - \tilde{\varphi}) + \gamma_i [\nabla_x - \nabla_i u^{(\nu)} + \nabla_{\nu} (\nabla_i v^{(\nu)})] + \alpha_i [\langle u^{(\nu)} \nabla_x (\nabla_i \varphi^{(\nu)}) \rangle_x \\ + \langle v^{(\nu)} \nabla_{\nu} (\nabla_i \varphi^{(\nu)}) \rangle_{\nu}] - \alpha \nabla^2 \varphi^{(\nu)} = R_{\varphi}^{(\nu)} \end{aligned} \quad (18)$$

$$\begin{aligned} \tilde{\gamma}(u^{(\nu)} - \tilde{u}) + \alpha_i \langle \varphi^{(\nu)} \rangle_x \nabla_x (\nabla_i \varphi^{(\nu)}) - \gamma_i f \langle \nabla_i v^{(\nu)} \rangle \\ + \gamma_i [\bar{\nabla}_x \langle u^{(\nu)} (\nabla_i u^{(\nu)}) \rangle + \bar{\nabla}_{\nu} \langle v^{(\nu)} \rangle (\nabla_i u^{(\nu)}) - (\nabla_i u^{(\nu)}) \bar{\nabla}_x u^{(\nu)} \\ - \langle (\nabla_i v^{(\nu)}) \nabla_x v^{(\nu)} \rangle] - \gamma_u \nabla^2 u^{(\nu)} = R_u^{(\nu)} \end{aligned} \quad (19)$$

and

$$\begin{aligned} \tilde{\gamma}(v^{(\nu)} - \tilde{v}) + \alpha_i \langle \varphi^{(\nu)} \rangle_{\nu} \nabla_{\nu} (\nabla_i \varphi^{(\nu)}) + \gamma_i f \langle \nabla_i v^{(\nu)} \rangle \\ + \gamma_i [\bar{\nabla}_x \langle u^{(\nu)} (\nabla_i v^{(\nu)}) \rangle + \bar{\nabla}_{\nu} \langle v^{(\nu)} \rangle (\nabla_i v^{(\nu)}) \\ - \langle (\nabla_i u^{(\nu)}) \bar{\nabla}_{\nu} u^{(\nu)} \rangle - (\nabla_i v^{(\nu)}) \bar{\nabla}_{\nu} v^{(\nu)}] - \gamma_v \nabla^2 v^{(\nu)} = R_v^{(\nu)}. \end{aligned} \quad (20)$$

In these equations, the finite time difference terms of the ν th guess, $\nabla_i \varphi^{(\nu)}$, $\nabla_i u^{(\nu)}$, and $\nabla_i v^{(\nu)}$, are equal to the right-hand sides of eq (12), (13), and (14) after substitution of φ , u , and v by $\varphi^{(\nu)}$, $u^{(\nu)}$, and $v^{(\nu)}$ as

$$\nabla_i \varphi^{(\nu)} = -\nabla_x \langle (\varphi^{(\nu)}) u^{(\nu)} \rangle - \nabla_{\nu} \langle (\varphi^{(\nu)}) v^{(\nu)} \rangle, \quad (21)$$

$$\nabla_i u^{(\nu)} = f \langle v^{(\nu)} \rangle - \nabla_x \varphi^{(\nu)} - (u^{(\nu)} \bar{\nabla}_x u^{(\nu)} + v^{(\nu)} \bar{\nabla}_{\nu} u^{(\nu)}), \quad (22)$$

and

$$\nabla_i v^{(\nu)} = -f \langle u^{(\nu)} \rangle - \nabla_{\nu} \varphi^{(\nu)} - \langle (u^{(\nu)}) \bar{\nabla}_x v^{(\nu)} \rangle + v^{(\nu)} \bar{\nabla}_{\nu} v^{(\nu)}. \quad (23)$$

The residual eq (18), (19), and (20) are nonlinear, but a simple correction technique is used to obtain the $(\nu+1)$ th guess field. The technique is to linearize the residual equations and then to collect only the terms that represent the values at the grid point where the corrections are to be made. To linearize eq (12) through (17), one assumes that the undisturbed field is a motionless fluid with a constant depth H and that small perturbations u , v , and φ are superimposed upon the undisturbed field. The linearized equations that correspond to eq (12), (13), and (14) are

$$\nabla_i \varphi^{(\nu)} = -\Phi (\nabla_x u^{(\nu)} + \nabla_{\nu} v^{(\nu)}), \quad (24)$$

$$\nabla_i u^{(\nu)} = f \langle v^{(\nu)} \rangle - \nabla_x \varphi^{(\nu)}, \quad (25)$$

and

$$\nabla_i v^{(\nu)} = -f \langle u^{(\nu)} \rangle - \nabla_{\nu} \varphi^{(\nu)}. \quad (26)$$

The linearized residual equations corresponding to eq (15),

(16), and (17) are

$$\tilde{\alpha}(\varphi^{(\nu)} - \tilde{\varphi}) + \alpha_i (\nabla_x \nabla_i u^{(\nu)} + \nabla_{\nu} \nabla_i v^{(\nu)}) + \alpha \nabla^2 \varphi^{(\nu)} = R_{\varphi}^{(\nu)}, \quad (27)$$

$$\tilde{\gamma}(u^{(\nu)} - \tilde{u}) + \alpha_i \Phi \nabla_x \nabla_i \varphi^{(\nu)} - \gamma_i f \langle \nabla_i v^{(\nu)} \rangle + \gamma_u \nabla^2 u^{(\nu)} = R_u^{(\nu)}, \quad (28)$$

and

$$\tilde{\gamma}(v^{(\nu)} - \tilde{v}) + \alpha_i \Phi \nabla_{\nu} \nabla_i \varphi^{(\nu)} + \gamma_i f \langle \nabla_i u^{(\nu)} \rangle + \gamma_v \nabla^2 v^{(\nu)} = R_v^{(\nu)}. \quad (29)$$

When considering only those terms given at a grid point and concerned with a variable the same as the major variable in each residual equation, that is, φ in R_{φ} , etc., the $(\nu+1)$ th values are

$$\varphi^{(\nu+1)} = \varphi^{(\nu)} - R_{\varphi}^{(\nu)} / D_{\varphi}, \quad (30)$$

$$u^{(\nu+1)} = u^{(\nu)} - R_u^{(\nu)} / D_u, \quad (31)$$

and

$$v^{(\nu+1)} = v^{(\nu)} - R_v^{(\nu)} / D_v \quad (32)$$

where

$$D_{\varphi} = \tilde{\alpha} + 4(\gamma_i + \alpha) \frac{1}{(2\Delta s)^2}, \quad (33)$$

$$D_u = \tilde{\gamma} + \gamma_i \frac{f^2}{4} + 2\alpha_i \frac{\Phi^2}{(2\Delta s)^2} + \gamma_u \frac{4}{(2\Delta s)^2}, \quad (34)$$

and

$$D_v = \tilde{\gamma} + \gamma_i \frac{f^2}{4} + 2\alpha_i \frac{\Phi^2}{(2\Delta s)^2} + \gamma_v \frac{4}{(2\Delta s)^2} \quad (35)$$

where Δs is an average grid size. As easily seen, this correction procedure is the simplest one among those that could be considered.

6. CONVERGENCE OF SOLUTION

Convergence of solution is investigated in this section (Todd 1962). Finite-difference equations used are linear and given in eq (24) through (35). Now, the amplification matrix \mathbf{G} is defined as

$$\begin{pmatrix} \Delta \varphi^{(\nu+1)} \\ \Delta u^{(\nu+1)} \\ \Delta v^{(\nu+1)} \end{pmatrix} = \mathbf{G} \begin{pmatrix} \Delta \varphi^{(\nu)} \\ \Delta u^{(\nu)} \\ \Delta v^{(\nu)} \end{pmatrix} \quad (36)$$

where $\Delta \varphi$, Δu , and Δv are the differences between the guess and true value,

$$\Delta \varphi^{(\nu+1)} = \varphi^{(\nu+1)} - \varphi, \quad \Delta u^{(\nu+1)} = u^{(\nu+1)} - u, \quad \Delta v^{(\nu+1)} = v^{(\nu+1)} - v, \quad (37)$$

and similar ones for $\Delta \varphi^{(\nu)}$, $\Delta u^{(\nu)}$, and $\Delta v^{(\nu)}$. The differences are assumed in a simple harmonic form

$$\begin{pmatrix} \Delta \varphi^{(\nu)} \\ \Delta u^{(\nu)} \\ \Delta v^{(\nu)} \end{pmatrix} = \begin{pmatrix} \varphi^* \\ u^* \\ v^* \end{pmatrix} e^{ikx + i\nu y}. \quad (38)$$

The operators Δ_x , ∇_{ν} , and $\langle \rangle$ appearing in eq (24) through (29) are replaced by the constants $i \sin k\Delta s / \Delta s$, $i \sin h\Delta s / \Delta s$, and $(\cos k\Delta s + \cos h\Delta s) / 2$, respectively, where $i = \sqrt{-1}$. Finally, the eigenvalues of the amplification matrix \mathbf{G} are obtained from the cubic equation

$$AG^3 + BG^2 + CG + D = 0, \quad (39)$$

and the criterion of convergence is given by

$$|G| \leq 1. \quad (40)$$

Some details of the above mathematical derivation are given in appendix 4.

Figures 2 and 3 are made to illustrate the characteristics of $|G|$ for various choices of weights. For convenience, the prime terms of nondimensional weights are defined as

$$\begin{aligned} \tilde{\alpha}' &= \frac{\alpha'_p}{a_p^2}, \\ \tilde{\gamma}' &= \frac{\gamma'_w}{a_w^2}, \\ \alpha'_i &= \frac{\alpha'_i}{a_p^2} (2\Delta t)^2, \\ \gamma'_i &= \frac{\gamma'_i}{a_w^2} (2\Delta t)^2, \\ \alpha' &= \frac{\alpha'}{a_p^2} (2\Delta s)^2, \\ \gamma'_u &= \frac{\gamma'_u}{a_w^2} (2\Delta s)^2, \end{aligned}$$

and

$$\gamma'_v = \frac{\gamma'_v}{a_w^2} (2\Delta s)^2$$

where a_p and a_w are the average amplitudes of geopotential fluctuation and wind velocity, respectively, and are taken as $a_p = g \times 100$ m and $a_w = 10$ m sec⁻¹. The values of the constants that appear in the calculation of $|G|$ are taken as $g = 9.8$ m sec⁻², $H = 10$ km, $f = 0.8365 \times 10^{-4}$ sec⁻¹, $\Delta t = 60$ sec, and $\Delta s = 200$ km. If Δt is taken as 10 min, α'_i and γ'_i are increased by 10^2 .

Figure 2 is made under the assumptions that the auxiliary terms α' , γ'_u , and γ'_v are infinitesimal, defining two ratios

$$\frac{\tilde{\gamma}'}{\tilde{\alpha}'} = \frac{\gamma'_i}{\alpha'_i} \left(\equiv \frac{\text{WIND}}{\text{PRESS}} \right)$$

and

$$\frac{\alpha'_i}{\tilde{\alpha}'} = \frac{\gamma'_i}{\tilde{\gamma}'} \left(\equiv \frac{\text{DYN}}{\text{OBS}} \right).$$

The amplification $|G|$ is shown as a function of these two ratios, namely, WIND/PRESS and DYN/OBS. The domain marked by a letter of CONV (convergence) where $|G| \leq 1$ shows the conditions of these ratios to obtain a converging solution by the iterative method described previously. The domain marked by a letter of DIV (divergence) where $|G| > 1$ shows the conditions under which no converging solution will be obtained. These two domains are divided by a solid curve marked by 1. It is interesting to note that convergence of solution will be achieved by giving more weight on wind terms than pressure terms or less weight on dynamical constraints than observational terms. Also, one of the other significant

characteristics shown in this figure is that the two domains are sharply divided, $|G|$ reaching its maximum value about 3.0 near the critical curve and remaining uniform in the domain of divergence. In the domain of convergence, similar characteristics are observed. The value of $|G|$ decreases rapidly, moving away from the critical curve, except for the region of higher ratio of WIND/PRESS.

For demonstrating the role of auxiliary low-pass filters on convergence, figure 3 is made under the assumptions that

$$\frac{\alpha'}{\tilde{\alpha}'} = \frac{\gamma'_u}{\tilde{\gamma}'} = \frac{\gamma'_v}{\tilde{\gamma}'} \left(\equiv \frac{\text{AUX}}{\text{OBS}} \right)$$

and

$$\frac{\alpha'_i}{\tilde{\alpha}'} = \frac{\gamma'_i}{\tilde{\gamma}'} \left(\equiv \frac{\text{DYN}}{\text{OBS}} \right).$$

From these conditions, easily seen is the relationship

$$\frac{\tilde{\gamma}'}{\tilde{\alpha}'} = \frac{\gamma'_u}{\alpha'} = \frac{\gamma'_v}{\alpha'} = \frac{\gamma'_i}{\alpha'_i}.$$

Therefore in figure 3, the ratio WIND/PRESS is a constant that is 1. In figure 3, the values of $|G|$ become independent with the ratio AUX/OBS as the ratio decreases and vary only with the ratio DYN/OBS. Accordingly, the condition of $|G|$ in figure 2 for the case where the ratio WIND/PRESS=1 is similar to the condition in figure 3 where the ratio AUX/OBS=10⁻³. It is seen also from figure 3 that solution converges more easily with a higher ratio of AUX/OBS.

Suppose we plan in the analysis to take the conditions WIND/PRESS=1 and DYN/OBS=10². These conditions will result in no converging solution if the auxiliary terms are taken as infinitesimal as seen from figure 2. However, if the auxiliary terms are taken so as to make the ratio AUX/OBS greater than 10, we may be able to obtain a converging solution as seen from figure 3.

The above discussion is based on the linearized set of equations. In practice, however, the residual equations are nonlinear, and further complications should be anticipated. In the following sections, numerical tests will be described for solving the nonlinear residual equations.

7. NUMERICAL TESTS

For testing the method, the observations of the geopotential $\tilde{\phi}$ and the wind components \tilde{u} and \tilde{v} are assumed to be given at all grid points, 16×16 points for $\tilde{\phi}$, 15×16 points for \tilde{u} , and 16×15 points for \tilde{v} . For simplicity, a simple harmonic wave expressed by a fluctuation of meridional motion is assumed to superimpose upon a uniform easterly current. This situation is represented by the numerical example

$$\tilde{u} = -10 \text{ m sec}^{-1} \quad \text{for } i = 1 \sim 15, j = 1 \sim 16$$

$$\tilde{v} = 5 \sin 2\pi(i-1)/15 \sin \pi(j-1)/14 \quad \text{for } i = 1 \sim 16, j = 1 \sim 15,$$

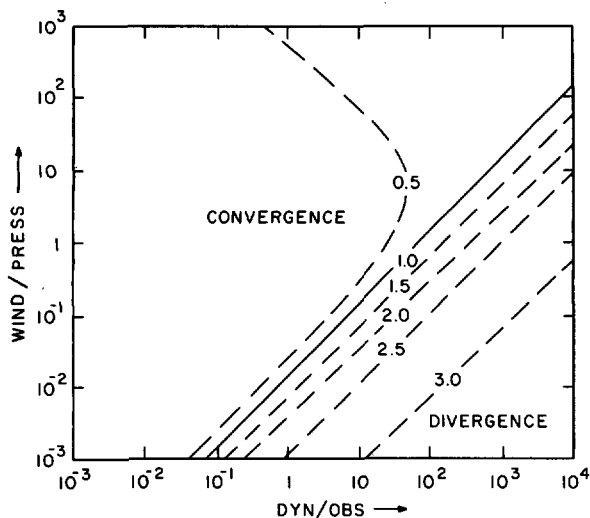


FIGURE 2.—Amplification rate $|G|$ for the case where the auxiliary terms α , γ_u , and γ_v are infinitesimal: $WIND/PRESS = \tilde{\gamma}'/\tilde{\alpha}' = \gamma'_u/\alpha'_u$ and $DYN/OBS = \alpha'_i/\tilde{\alpha}' = \gamma'_i/\tilde{\gamma}'$ where the primed quantities are nondimensional weights. (PRESS is pressure; DYN, dynamics; and OBS, observations.)

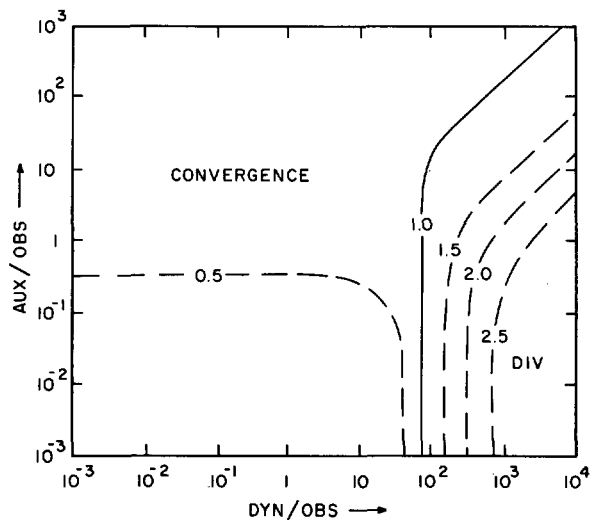


FIGURE 3.—Amplification rate G for the case where the auxiliary terms are finite: $AUX/OBS = \alpha'_i/\tilde{\alpha}' = \gamma'_u/\tilde{\gamma}' = \gamma'_v/\tilde{\gamma}'$ and $DYN/OBS = \alpha'_i/\tilde{\alpha}' = \gamma'_i/\tilde{\gamma}'$.

and $\tilde{\varphi}$ is calculated from the finite-difference equations representing the geostrophic wind relationship

$$\begin{aligned} \tilde{\varphi}_{i,j-1} - \tilde{\varphi}_{i,j} &= f2\Delta y \tilde{u}_{i,j} \\ \tilde{\varphi}_{i+1,j} - \tilde{\varphi}_{i,j} &= f2\Delta x \tilde{v}_{i,j}, \end{aligned}$$

assuming $\tilde{\varphi}_{11} = \Phi$. Numerical values for the constants are $\Delta t = 5$ min, $\Delta x = \Delta y = \Delta z = 200$ km, $f = 0.6 \times 10^{-4}$ sec⁻¹, $\Phi = 9.8$ m sec⁻² $\times 10$ km. The weights chosen are equivalent to the conditions expressed by $WIND/PRESS = 1.0$ and $DYN/OBS = 25$ in figure 2 that satisfy the convergence criterion. The auxiliary terms are initially set to be zero and increase whenever the tendency of diverging solution

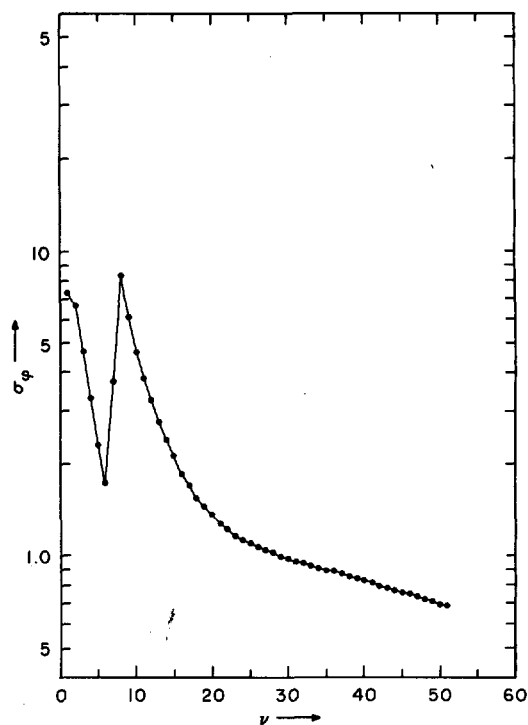


FIGURE 4.—Standard deviation σ_φ of $(\nabla_t \varphi \cdot 2\Delta t)$ as a function of the number of iterations ν , case (1).

appears. The convergence of the method is tested for two cases:

1. Initial guess is the observed value, geostrophic, $u^{(0)} = \tilde{u}$, $v^{(0)} = \tilde{v}$, and $\varphi^{(0)} = \tilde{\varphi}$.
2. Initial guess is that $u^{(0)} = v^{(0)} = \varphi^{(0)} = 0$ except that the observed values, geostrophic, are used for the initial guess at the boundary,

$$\begin{aligned} u_{1,j}^{(0)} &= \tilde{u}_{1,j} \text{ and } u_{15,j}^{(0)} = \tilde{u}_{15,j} & \text{for } j=1 \sim 16 \\ u_{i,1}^{(0)} &= \tilde{u}_{i,1} \text{ and } u_{i,16}^{(0)} = \tilde{u}_{i,16} & \text{for } i=1 \sim 15. \end{aligned}$$

Similarly, $v^{(0)}$ and $\varphi^{(0)}$ are given at the boundary.

The results of cases (1) and (2) are shown in figures 4 through 9. A measure of testing the method is to check whether or not the solution converges and how closely the solution satisfies the steadiness condition (4). The convergence rate can be seen in these figures in which the errors are defined as

$$\sigma_\varphi = \left[\frac{1}{N_\varphi} \sum_{i,j} (\nabla_t \varphi \cdot 2\Delta t)^2 \right]^{1/2}, \tag{41}$$

$$\sigma_u = \left[\frac{1}{N_u} \sum_{i,j} (\nabla_t u \cdot 2\Delta t)^2 \right]^{1/2}, \tag{42}$$

and

$$\sigma_v = \left[\frac{1}{N_v} \sum_{i,j} (\nabla_t v \cdot 2\Delta t)^2 \right]^{1/2} \tag{43}$$

where σ_φ , σ_u , and σ_v are the standard deviations; N_φ ($= 16 \times 16$), N_u ($= 15 \times 16$), and N_v ($= 16 \times 15$) are total

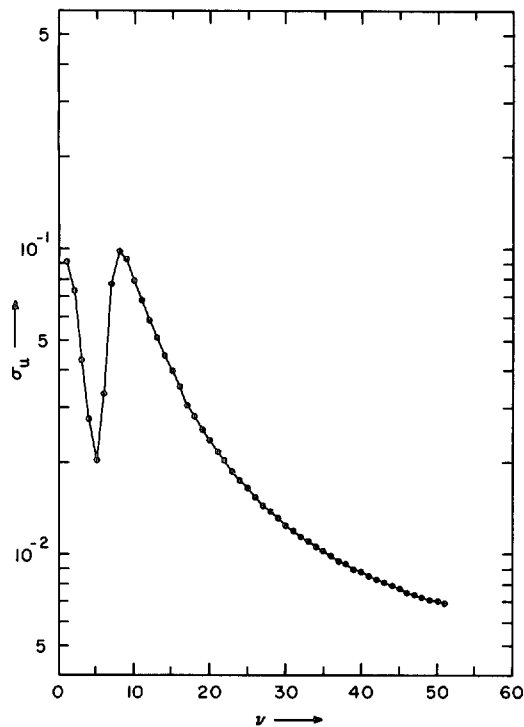


FIGURE 5.—Standard deviation σ_u of $(\nabla_t u \cdot 2\Delta t)$ as a function of the number of iterations ν , case (1).

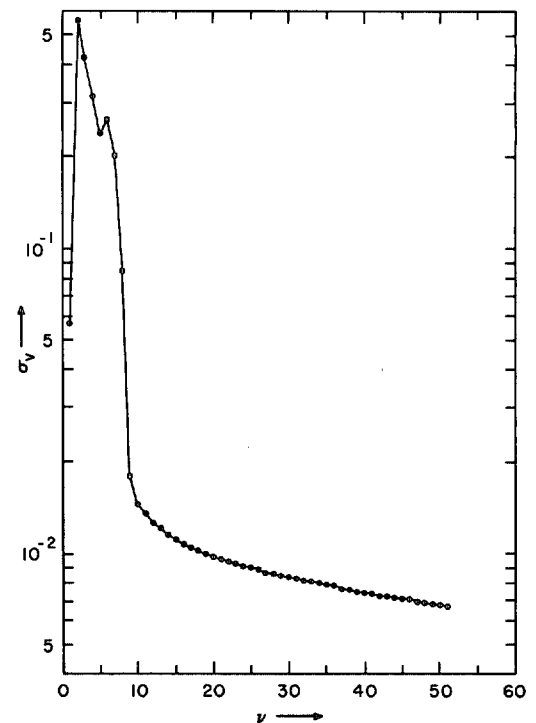


FIGURE 6.—Standard deviation σ_v of $(\nabla_t v \cdot 2\Delta t)$ as a function of the number of iterations ν , case (1).

grid points assigned for each variable; and $2\Delta t$ is multiplied to each time change term for convenience.

CASE (1)

The geostrophic wind relationship is assumed for the observed values $\tilde{\varphi}$, \tilde{u} , and \tilde{v} . The initial guess values $\varphi^{(0)}$, $u^{(0)}$, and $v^{(0)}$ are taken to be the same as the observed. Figures 4, 5, and 6 represent respectively the variations of σ_φ , σ_u and σ_v as functions of the number of iterations.

It is interesting to note that, in the first several steps of iteration in the φ and u fields, the initial standard deviations decrease. However, the initial standard deviations in the v field increase. From a number of the tests made, which were not described in this article, it was found, in general, that the standard deviations σ_φ , σ_u , and σ_v decrease in the first several or a few 10 steps of iteration and then increase to a level considerably higher than the lowest level of the standard deviations obtained in the preceding steps of iteration. This increase is abrupt, as clearly seen in figure 4. Similar behavior was also observed in the standard deviations of R_φ , R_u , and R_v . The reason for this increase has not been found. However, it is probably due to an unpredicted divergence of solution caused by the nonlinearity of the residual equations. Another possible reason is the relatively slow convergence rate of the Richardson method compared with the other method. Also, the correction forms (30)~(35) used in the relaxation may be too simple to make the desirable convergence. It is apparent, however, that the increase of

the standard deviations is difficult to understand without considering the nonlinearity. Due to the nonlinearity, the iteration method should be improved on a "trial and error" basis because of analytical difficulties involved in nonlinear equations. Otherwise, it is necessary to use the analyzed values of φ , u , and v at the iteration step of the minimum standard deviations before they jump to higher values.

A technique proposed in this study is to add the auxiliary terms α , γ_u , and γ_v to the functional as seen in eq (11). The weight of auxiliary terms should be kept minimal. The weights α , γ_u , and γ_v are increased whenever the tendency of divergence appears in the iterative process. These terms contribute as a damping factor in the iterative process. From the viewpoint of the objective analysis method, the technique is optional but was useful, namely by smoothing the field, not changing the relative weights between the observations and the dynamical constraints, we were able to obtain the solution that satisfied the conditions

$$(\nabla_t \varphi)^2 \rightarrow 0, \quad (\nabla_t u)^2 \rightarrow 0, \quad \text{and} \quad (\nabla_t v)^2 \rightarrow 0.$$

The results shown in figures 4, 5, and 6 are those in which this technique is used to obtain proper converging solutions. In figure 4, σ_φ starts to increase at the sixth iteration step and continues to increase at the seventh step. After reaching the maximum at the eighth iteration step, σ_φ continuously decreases. A similar process is seen also in figure 5, except that the minimum occurs at the fourth iteration and the maximum occurs at the seventh iteration. In figure 6, the first minimum is at the first

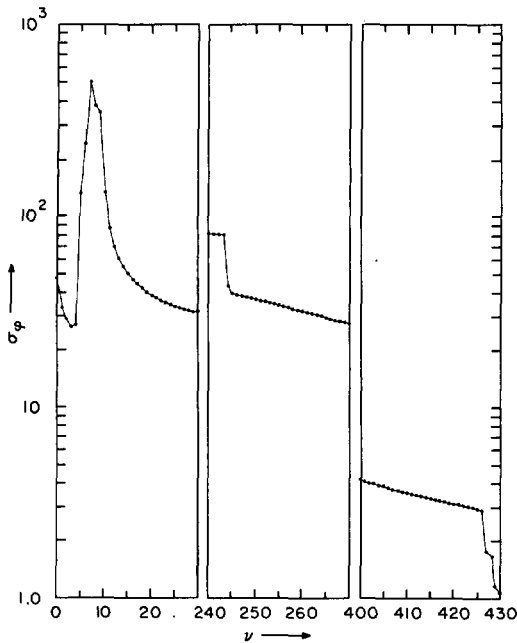


FIGURE 7.—Standard deviation σ_ϕ of $(\nabla_t \phi \cdot 2\Delta t)$ as a function of the number of iterations ν , case (2).

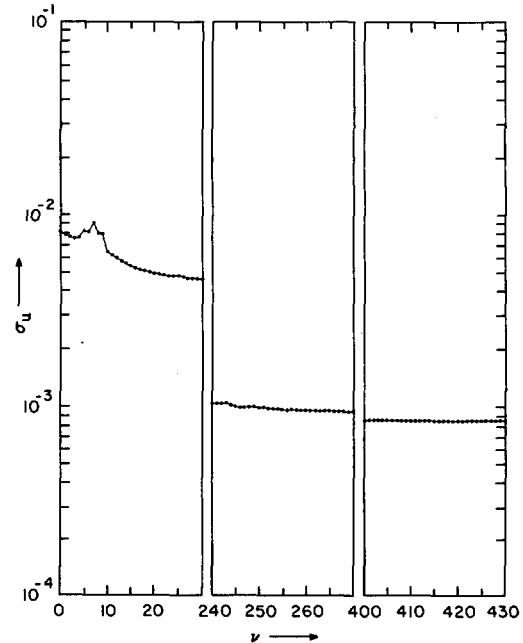


FIGURE 8.—Standard deviation σ_u of $(\nabla_t u \cdot 2\Delta t)$ as a function of the number of iterations ν , case (2).

iteration after iteration starts; and the first maximum occurs at the second iteration step. Lags of iteration steps of the minimum and maximum among the three fields ϕ , u , and v may imply that the ϕ field is first well relaxed while the u and v fields accumulate the errors and then the u and v fields follow. The values of α , γ_u , and γ_v are given in table 1 in which, for convenience, the non-dimensional auxiliary weights α' , γ'_u , and γ'_v are listed for each step of iteration.

CASE (2)

The only difference in this case from case (1) is that the initial guess of this case is taken as $\phi^{(0)}=0$, $u^{(0)}=0$, and $v^{(0)}=0$ at all interior grid points, except those at the boundary. The iteration continued up to 1000 steps. Figures 7, 8, and 9 show the standard deviations for selected portions of the iteration steps where significant change occurred in one of the standard deviations. Other portions show monotonic changes. Compared with case (1), slow convergence of solution is characteristic and almost 300 iteration steps are necessary to reduce all standard deviations less than one-tenth of the initial standard deviation.

The technique of adding the auxiliary terms in eq (11), as employed in this study, is a key to making the solution converge; this is seen by comparison of table 1 with table 2. Table 2 was made for case (2) in a way similar to table 1 for case (1). In this comparison, it is clearly noted that the poor initial guess in case (2) requires more weight in the auxiliary terms of eq (11) than the better initial guess in case (1). Use of a good initial guess is important if the technique is employed.

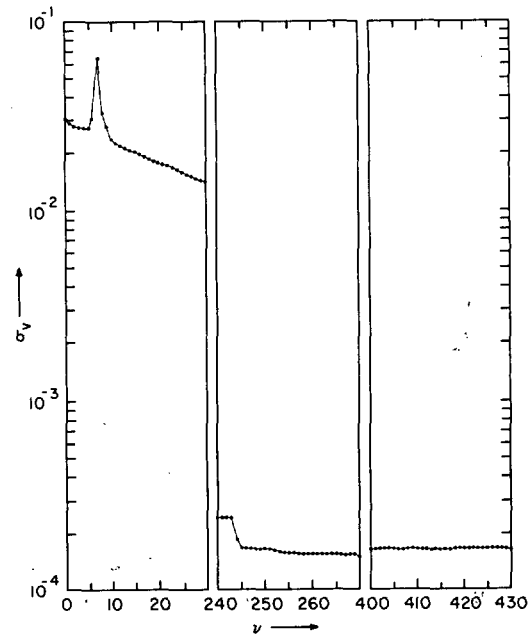


FIGURE 9.—Standard deviation σ_v of $(\nabla_t v \cdot 2\Delta t)$ as a function of the number of iterations ν , case (2).

8. APPLICATION TO HURRICANE DORA, 1964, OVER DATA-SPARSE AREAS

Another test of the method was made by analyzing the 500-mb height and wind data of hurricane Dora at 1200 GMT on Sept. 8, 1964, when the hurricane was approximately at 75° W., 28° N., 300 n.mi. due east of Cape Ken-

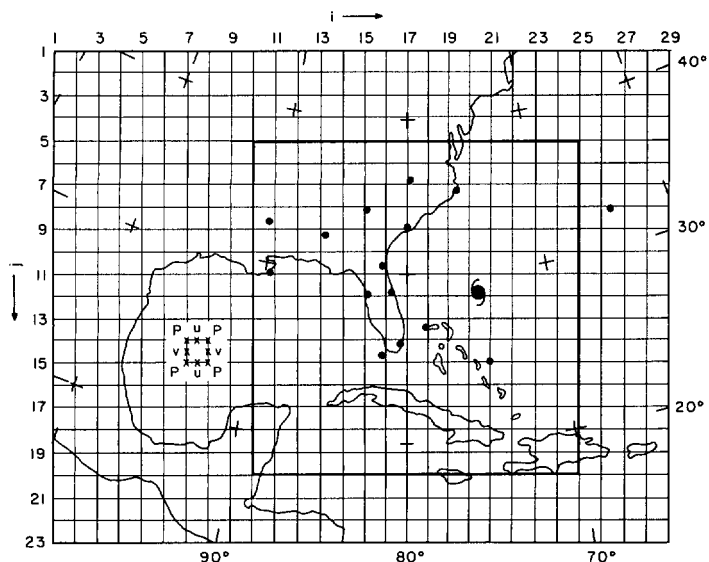


FIGURE 10.—Grid system and upper air stations used for objective analysis; the output is made only for the area indicated by the heavy line.

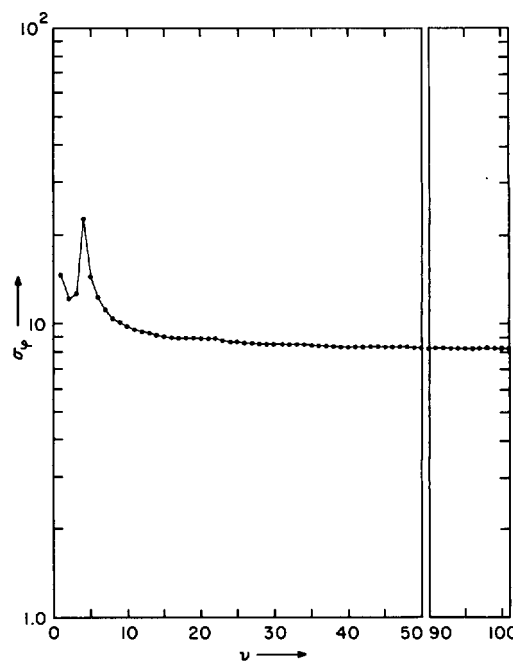


FIGURE 11.—Standard deviation σ_ϕ of $(\nabla_i \phi \cdot 2\Delta t)$ as a function of the number of iterations ν for the 500-mb data of hurricane Dora at 1200 GMT on Sept. 8, 1964.

speed. The geopotential anomaly is equivalent to a height anomaly of approximately 20 m because g is 9.8 m sec^{-2} . The height value and wind speed are of the same order as the analyzed ones (figs. 14, 15, and 16). Therefore, it will mean that the weights on wind terms are nearly the same as the weights given on the height terms in the equation of variation (11). This set of weights is the same as the tests in section 7. However, a major difference is given in the sets of input data, that is, the data in section 7 represent large scale only, and the data in section 8 are those affected by a systematic smaller scale (hurricane). Although high-frequency disturbances are filtered out by the dynamical constraints of vanishing $\nabla_i \phi$, $\nabla_i u$, and $\nabla_i v$, low-frequency patterns affected by the hurricane, such as divergence, may remain. In other words, the dynamical constraints on the wind velocity components described in (4), that is $\nabla_i u \neq 0$ and $\nabla_i v \neq 0$, are better satisfied than the constraint, $\nabla_i \phi \neq 0$. Indeed, this expectation is clearly demonstrated in figures 11, 12, and 13. In these figures, the ordinate represents the number of iterations, and the abscissa indicates the standard deviation of $\nabla_i \phi$, $\nabla_i u$, and $\nabla_i v$ calculated over the entire grid points. All of these standard deviations are lessened as the number of iterations increases due to the proposed self-controlled convergence technique. After 100 iterations, the standard deviation of $\nabla_i \phi$, σ_ϕ decreases to half of the initial value (fig. 11) while the standard deviations of $\nabla_i u$ and $\nabla_i v$, σ_u and σ_v , respectively, decrease to about 2 percent of the initial values. Therefore, at the end of iteration, the above set of weights does still allow certain magnitudes of divergence. The divergence pattern is given in figure 17 where the order of magnitude of divergence (10^{-5} sec^{-1}) seems to be reasonable.

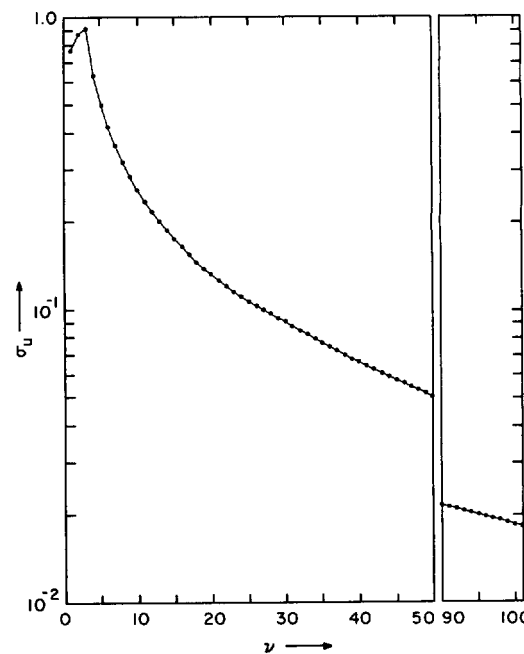


FIGURE 12.—Standard deviation σ_u of $(\nabla_i u \cdot 2\Delta t)$ as a function of the number of iterations ν for the 500-mb data of hurricane Dora at 1200 GMT on Sept. 8, 1964.

Figure 14 shows the analyzed height anomaly in meters. Other than the area near the hurricane center, the height pattern and its magnitudes are reasonably in agreement with the subjective analysis. Near the hurricane, the hurricane center obtained from the analysis and marked

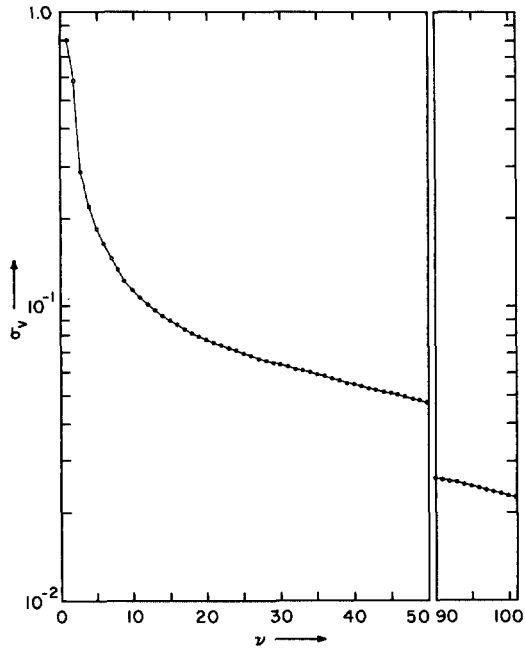


FIGURE 13.—Standard deviation σ_v of $(\nabla_i \psi \cdot 2\Delta t)$ as a function of the number of iterations ν for the 500-mb data of hurricane Dora at 1200 GMT on Sept. 8, 1964.

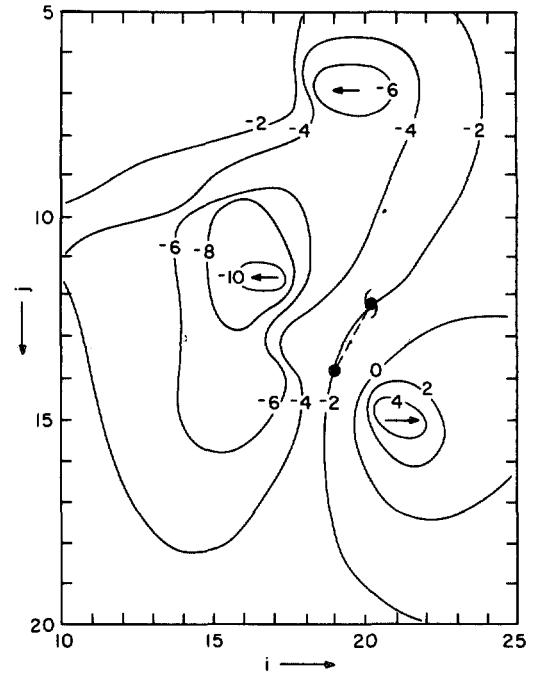


FIGURE 15.—The u component of wind for the 500-mb surface of hurricane Dora at 1200 GMT on Sept. 8, 1964, by the numerical variational objective analysis method.

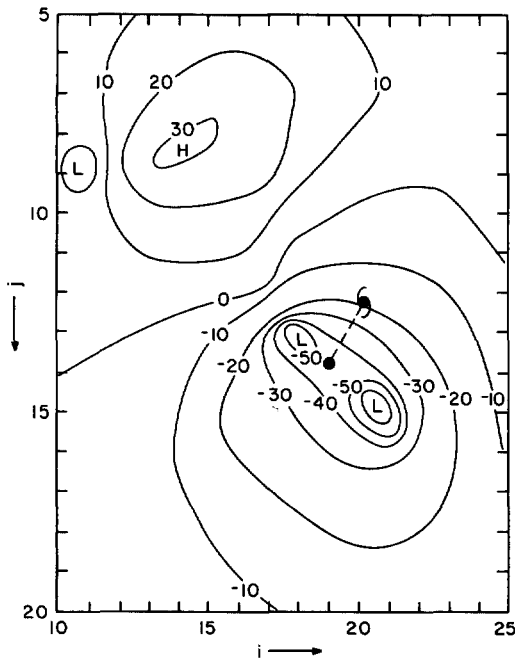


FIGURE 14.—Analyzed height pattern (units in meters) of the 500-mb pressure surface of hurricane Dora at 1200 GMT on Sept. 8, 1964, by the numerical variational objective analysis method.

by a dot in figures 14 through 17 seems to be a few hundred kilometers to the southwest compared with the officially reported position marked by a winged dot. Furthermore, the analysis shows two Low centers on the 500-mb surface, but one Low center seems more reasonable. These results are undesirable and seem to be caused

by the sparseness of data. Also, the nonuniform station density, higher westward and lower eastward, seems to result in the displacement of the analyzed hurricane center, westward.

Figures 15 and 16 show the u and v patterns, respectively. The magnitudes of u and v are not as great as one may expect near the hurricane on the 500-mb surface. However, they are reasonable in other areas. It is also interesting to note that stronger wind velocity components appear in the northwest quadrant than in other quadrants. This result is not verifiable, either due to data sparseness or for physical reasons. Figure 17 represents the divergence pattern calculated from the analyzed u and v . An interesting result is that a quadruple structure appeared in the hurricane area and a double system of divergence in the northwestern quadrant is stronger than the other one.

National Hurricane Research Laboratory (NHRL) reconnaissance aircraft data and analysis are available at three levels (9,800 ft, 11,780 ft, and 18,280 ft) on Sept. 8, 1964. Unfortunately, the data coverage is too small to compare with this study. The above results, however, may be compared with the subjective upper air analysis made by Sheets (1965). His analysis of the upper air sounding data is based on the hypothesis that the hurricane moved in the same direction with a constant velocity for the period of 1200 GMT on Sept. 7, 1964, through 0000 GMT on Sept. 12, 1964. Placing all upper air station data available at that period at the points relative to the hurricane center, he could generate 137 data points in a circular area with a 600-n.mi. radius around the hurricane center.

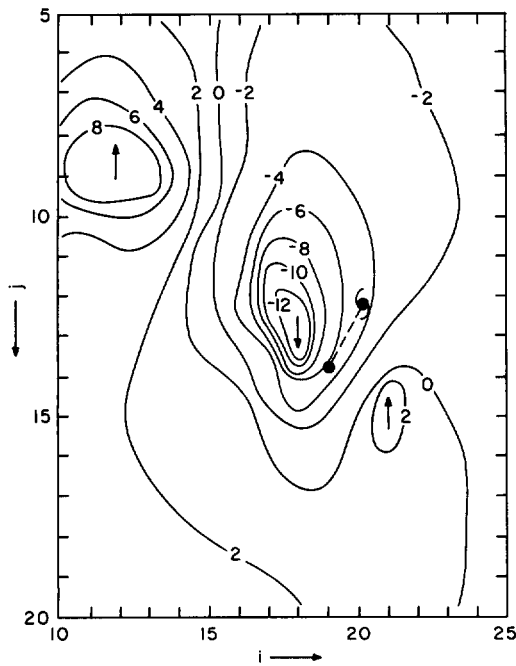


FIGURE 16.—The v component of wind for the 500-mb surface of hurricane Dora at 1200 GMT on Sept. 8, 1964, by the numerical variational objective analysis method.

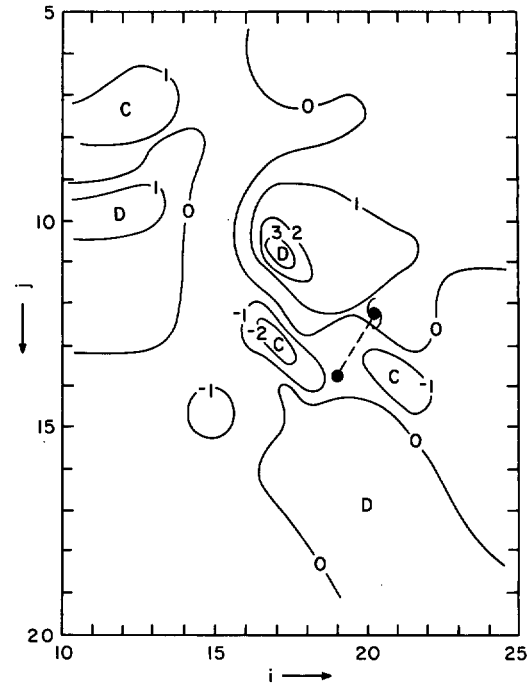


FIGURE 17.—Divergence pattern (units, 10^{-5} sec^{-1}) calculated from the analyzed u and v by the finite-difference form $\nabla_x u + \nabla_y v$.

Because hurricane Dora, 1964, seemed to satisfy the hypothesis fairly well, Sheets' analyzed patterns are used for comparison with the results of this study. Elongation of a Low in a north-south direction is shown in the results of those two different analyses. Also, tighter contours in the southeastern quadrant are seen in both analyses. A two-cell structure does not appear in Sheets' analysis on the 500-mb surface, but it appears at 400 mb. Higher wind speed in the northwestern quadrant is seen in both analyses, and magnitudes of the speed and direction are also in good agreement.

APPENDIX 1, PROOF OF EQUATION (9)

A proof of eq (9) is as follows:

$$\begin{aligned} \sum \psi \langle \varphi \rangle_x &= \sum_i \psi_{i,j} \left(\frac{\varphi_{i+1,j} + \varphi_{i,j}}{2} \right) \\ &= \left\{ \dots + \frac{\psi_{i,j} \varphi_{i-1,j}}{2} + \frac{\psi_{i,j} \varphi_{i,j}}{2} + \frac{\psi_{i-1,j} \varphi_{i,j}}{2} \right. \\ &\quad \left. + \frac{\psi_{i-1,j} \varphi_{i-1,j}}{2} + \dots \right\} = \sum \langle \psi \rangle_x \varphi. \end{aligned}$$

The above proof is for one dimension, but can be extended easily for two-dimensional cases. Also, the above proof is made only for the interior points where the symmetry of operators concerning a grid point of consideration is apparent. The symmetry is not valid at the boundary, and a separate calculation should be made. It is possible, however, to choose a finite-difference form of the boundary condition that satisfies eq (9).

APPENDIX 2, DERIVATION OF RESIDUAL EQUATIONS

After performing the first step of the calculus of variations on eq (11), we obtain

$$\begin{aligned} \delta J = 2 \sum_{i,j} \{ &\tilde{\alpha}(\varphi - \tilde{\varphi}) \delta \varphi + \tilde{\gamma}(u - \tilde{u}) \delta u + \tilde{\gamma}(v - \tilde{v}) \delta v + \alpha_i \nabla_i \varphi \delta(\nabla_i \varphi) \\ &+ \gamma_i \nabla_i u \delta(\nabla_i u) + \gamma_i \nabla_i v \delta(\nabla_i v) + \alpha(\nabla_x \varphi \nabla_x \delta \varphi + \nabla_y \varphi \nabla_y \delta \varphi) \}. \end{aligned} \quad (44)$$

Taking variations of eq (12), (13), and (14), one may write the variations of time change terms $\delta(\nabla_i \varphi)$, $\delta(\nabla_i u)$, and $\delta(\nabla_i v)$ as

$$\delta(\nabla_i \varphi) = -[\nabla_x \langle \langle \varphi \rangle_x \delta u \rangle + \nabla_y \langle \langle \varphi \rangle_y \delta v \rangle + \nabla_x \langle \langle \delta \varphi \rangle_x \rangle + \nabla_y \langle \langle \delta \varphi \rangle_y \rangle], \quad (45)$$

$$\delta(\nabla_i u) = f \langle \delta v \rangle - \nabla_x \delta \varphi - (\bar{\nabla}_x u \cdot \delta u + u \bar{\nabla}_x \delta u + \bar{\nabla}_y u \cdot \langle \delta v \rangle + \langle v \rangle \bar{\nabla}_y \delta u), \quad (46)$$

and

$$\delta(\nabla_i v) = -f \langle \delta u \rangle - \nabla_y \delta \varphi - (\langle \delta u \rangle \bar{\nabla}_x v + \langle u \rangle \bar{\nabla}_x \delta v + \delta v \bar{\nabla}_y v + v \bar{\nabla}_y \delta v). \quad (47)$$

Substitution of eq (45), (46), and (47) into eq (44) leads to

$$\begin{aligned} \delta J = 2 \sum_{i,j} \{ &\tilde{\alpha}(\varphi - \tilde{\varphi}) \delta \varphi - \alpha_i (\nabla_i \varphi) [\nabla_x \langle \langle \varphi \rangle_x \delta u \rangle + \nabla_y \langle \langle \varphi \rangle_y \delta v \rangle] \\ &+ \nabla_x \langle \langle \delta \varphi \rangle_x u \rangle + \nabla_y \langle \langle \delta \varphi \rangle_y v \rangle + \alpha(\nabla_x \varphi \nabla_x \delta \varphi + \nabla_y \varphi \nabla_y \delta \varphi) + \tilde{\gamma}(u - \tilde{u}) \delta u \\ &+ \gamma_i (\nabla_i u) [f \langle \delta v \rangle - \nabla_x \delta \varphi - (\delta u \bar{\nabla}_x u + \langle \delta v \rangle \bar{\nabla}_y u + u \bar{\nabla}_x \delta u + \langle v \rangle \bar{\nabla}_y \delta u)] \\ &+ \gamma_u (\nabla_x u \nabla_x \delta u + \nabla_y u \nabla_y \delta u) + \tilde{\gamma}(v - \tilde{v}) \delta v + \gamma_v (\nabla_i v) [-f \langle \delta u \rangle - \nabla_y \delta \varphi \\ &- (\langle \delta u \rangle \bar{\nabla}_x v + \delta v \bar{\nabla}_y v + \langle u \rangle \bar{\nabla}_x \delta v + v \bar{\nabla}_y \delta v)] \} + \gamma_v (\nabla_x v \nabla_x \delta v + \nabla_y v \nabla_y \delta v). \end{aligned}$$

After using the commutation rules (9) and (10), the above equation becomes

$$\begin{aligned} \delta J = 2 \sum_{i,j} \{ & \delta\varphi[\tilde{\alpha}(\varphi - \tilde{\varphi}) + \alpha_i \langle (u \nabla_x (\nabla_i \varphi))_x + (v \nabla_y (\nabla_i \varphi))_y \rangle \\ & + \gamma_i (\nabla_x (\nabla_i u) + \nabla_y (\nabla_i v)) - \alpha \nabla^2 \varphi] \\ & + \delta u [\tilde{\gamma}(u - \tilde{u}) + \gamma_i (-f \langle \nabla_i v \rangle + (\bar{\nabla}_x \langle (\nabla_i u) u \rangle + \bar{\nabla}_y \langle (\nabla_i u) v \rangle) \\ & - (\nabla_i u) \bar{\nabla}_x u - \langle (\nabla_i v) \bar{\nabla}_x v \rangle) + \alpha_i \langle \varphi \rangle_x \nabla_x (\nabla_i \varphi) - \gamma_u \nabla^2 u] \\ & + \delta v [\tilde{\gamma}(v - \tilde{v}) + \gamma_i (f \langle \nabla_i u \rangle + \bar{\nabla}_x \langle (\nabla_i v) u \rangle + \bar{\nabla}_y \langle (\nabla_i v) v \rangle) \\ & - \langle (\nabla_i u) \bar{\nabla}_y u \rangle - \langle (\nabla_i v) \bar{\nabla}_y v \rangle + \alpha_i \langle \varphi \rangle_y \nabla_y (\nabla_i \varphi) - \gamma_v \nabla^2 v] \}. \end{aligned} \quad (48)$$

For satisfying the extremum condition $\delta J = 0$ for arbitrary variations of $\delta\varphi$, δu , and δv , the coefficients of $\delta\varphi$, δu , and δv of eq (48) should vanish separately; that leads to eq (15), (16), and (17).

APPENDIX 3, CHARACTERISTIC CONDITION

It is desirable to solve eq (15), (16), and (17) as a boundary problem. For checking the possibility, a limiting case where Δt , Δx , and Δy approach zero is considered. Also, for simplicity, linearization is used. The linearized equations that correspond to eq (12), (13), and (14) under the above conditions are

$$\frac{\partial \varphi}{\partial t} = -\Phi \left(\frac{\partial u}{\partial x} + \frac{\partial v}{\partial y} \right), \quad (49)$$

$$\frac{\partial u}{\partial t} = f v - \frac{\partial \varphi}{\partial x}, \quad (50)$$

and

$$\frac{\partial v}{\partial t} = -f u - \frac{\partial \varphi}{\partial y}. \quad (51)$$

Similarly, the linearized equations corresponding to eq (15), (16), and (17) are

$$\tilde{\alpha}(\varphi - \tilde{\varphi}) + \alpha_i \left[\frac{\partial}{\partial x} \left(\frac{\partial u}{\partial t} \right) + \frac{\partial}{\partial y} \left(\frac{\partial v}{\partial t} \right) \right] - \alpha \left(\frac{\partial^2 \varphi}{\partial x^2} + \frac{\partial^2 \varphi}{\partial y^2} \right) = 0, \quad (52)$$

$$\tilde{\gamma}(u - \tilde{u}) + \alpha_i \Phi \frac{\partial}{\partial x} \left(\frac{\partial \varphi}{\partial t} \right) - \gamma_i f \frac{\partial v}{\partial t} - \gamma_u \left(\frac{\partial^2 u}{\partial x^2} + \frac{\partial^2 u}{\partial y^2} \right) = 0, \quad (53)$$

and

$$\tilde{\gamma}(v - \tilde{v}) + \alpha_i \Phi \frac{\partial}{\partial y} \left(\frac{\partial \varphi}{\partial t} \right) + \gamma_i f \frac{\partial u}{\partial t} - \gamma_v \left(\frac{\partial^2 v}{\partial x^2} + \frac{\partial^2 v}{\partial y^2} \right) = 0. \quad (54)$$

When rearranging the terms in the order of higher derivatives, substitution of eq (49), (50), and (51) into eq (52), (53), and (54) will lead to the set of equations

$$-(\alpha + \alpha_i) \left(\frac{\partial^2 \varphi}{\partial x^2} + \frac{\partial^2 \varphi}{\partial y^2} \right) + \alpha_i f \left(\frac{\partial v}{\partial x} - \frac{\partial u}{\partial y} \right) + \tilde{\alpha}(\varphi - \tilde{\varphi}) = 0, \quad (55)$$

$$\begin{aligned} -(\gamma_u + \alpha_i \Phi^2) \frac{\partial^2 u}{\partial x^2} - \gamma_u \frac{\partial^2 u}{\partial y^2} - \alpha_i \Phi^2 \frac{\partial^2 v}{\partial x \partial y} + \gamma_i f \frac{\partial \varphi}{\partial y} \\ + \gamma_i f^2 u + \tilde{\gamma}(u - \tilde{u}) = 0, \end{aligned} \quad (56)$$

$$\begin{aligned} -\alpha_i \Phi^2 \frac{\partial^2 u}{\partial x \partial y} - \gamma_v \frac{\partial^2 v}{\partial x^2} - (\gamma_v + \alpha_i \Phi^2) \frac{\partial^2 v}{\partial y^2} - \gamma_i f \frac{\partial \varphi}{\partial x} \\ + \gamma_i f^2 v + \tilde{\gamma}(v - \tilde{v}) = 0. \end{aligned} \quad (57)$$

The question of whether or not the above equations can be solved as a boundary value problem will be investigated by the method of characteristics (Courant and Hilbert 1962). We consider a line C , $\xi(x,y) = 0$, along which the first derivatives of solutions φ , u , and v are continuous, but the second derivatives may suffer jump discontinuity across C .

By taking another function, $\eta(x,y)$, orthogonal to ξ , one may transform the derivatives from the (x, y) plane to the (ξ, η) plane as

$$\frac{\partial \varphi}{\partial x} = \frac{\partial \varphi}{\partial \xi} \frac{\partial \xi}{\partial x} + \frac{\partial \varphi}{\partial \eta} \frac{\partial \eta}{\partial x} + \dots,$$

$$\frac{\partial^2 \varphi}{\partial x^2} = \frac{\partial^2 \varphi}{\partial \xi^2} \left(\frac{\partial \xi}{\partial x} \right)^2 + \dots,$$

and

$$\frac{\partial^2 u}{\partial x \partial y} = \frac{\partial^2 u}{\partial \xi^2} \frac{\partial \xi}{\partial x} \frac{\partial \xi}{\partial y} + \dots$$

Similar expressions are given to the other derivatives appearing in eq (55), (56), and (57). After substituting the above expressions into eq (55), (56), and (57), the characteristic condition will be derived from the condition that the determinant, elements of which are the coefficients of $\partial^2 \varphi / \partial \xi^2$, $\partial^2 u / \partial \xi^2$, and $\partial^2 v / \partial \xi^2$, vanishes so that these second derivatives have no unique solution. The characteristic condition is

$$\Delta = \begin{vmatrix} -(\alpha + \alpha_i) \left[\left(\frac{\partial \xi}{\partial x} \right)^2 + \left(\frac{\partial \xi}{\partial y} \right)^2 \right], & 0, & 0 \\ 0, & -\alpha_i \Phi^2 \left(\frac{\partial \xi}{\partial x} \right)^2 - \gamma_u \left[\left(\frac{\partial \xi}{\partial x} \right)^2 + \left(\frac{\partial \xi}{\partial y} \right)^2 \right], & -\alpha_i \Phi^2 \frac{\partial \xi}{\partial x} \frac{\partial \xi}{\partial y} \\ 0, & -\alpha_i \Phi^2 \frac{\partial \xi}{\partial x} \frac{\partial \xi}{\partial y}, & -\alpha_i \Phi^2 \left(\frac{\partial \xi}{\partial y} \right)^2 - \gamma_v \left[\left(\frac{\partial \xi}{\partial x} \right)^2 + \left(\frac{\partial \xi}{\partial y} \right)^2 \right] \end{vmatrix} = 0,$$

or

$$\begin{aligned} \Delta = (\alpha + \alpha_i) \left[\left(\frac{\partial \xi}{\partial x} \right)^2 + \left(\frac{\partial \xi}{\partial y} \right)^2 \right]^2 \left\{ \alpha_i \Phi^2 \left[\gamma_u \left(\frac{\partial \xi}{\partial y} \right)^2 \right. \right. \\ \left. \left. + \gamma_v \left(\frac{\partial \xi}{\partial x} \right)^2 \right] + \gamma_u \gamma_v \left[\left(\frac{\partial \xi}{\partial x} \right)^2 + \left(\frac{\partial \xi}{\partial y} \right)^2 \right] \right\}. \end{aligned} \quad (58)$$

Therefore, the characteristic condition will not be satisfied if $\partial \xi / \partial x$, $\partial \xi / \partial y$, γ_u and γ_v do not vanish,

$$\Delta \neq 0. \quad (59)$$

The auxiliary terms, especially the γ_u and γ_v terms in eq (11), may make it possible to solve the Euler eq (15), (16), and (17) as a boundary problem even though the auxiliary terms are small. In practice, the magnitudes of

α , γ_u , and γ_v are increased whenever the divergence of solution appears in the iterative process. This increase of the magnitude is taken due to nonlinearity of the Euler equations. A similar discussion is given in the author's articles (Sasaki 1970a, 1970b).

APPENDIX 4, CONVERGENCE OF SOLUTION

Substitution of eq (24) ~ (26) into (27) ~ (29) leads to

$$\begin{aligned} \tilde{\alpha}\Delta\varphi^{(v)} + \gamma_t\nabla_x(f\langle\Delta v^{(v)}\rangle - \nabla_x\Delta\varphi^{(v)}) + \gamma_t\nabla_y(-f\langle\Delta u^{(v)}\rangle - \nabla_y\Delta\varphi^{(v)}) - \alpha\nabla^2\Delta\varphi^{(v)} = R_\varphi^{(v)}, \end{aligned} \quad (60)$$

$$\begin{aligned} \tilde{\gamma}\Delta u^{(v)} + \alpha_t\Phi\nabla_x(-\Phi(\nabla_x\Delta u^{(v)} + \nabla_y\Delta v^{(v)})) - \gamma_t f\langle -f\langle\Delta u^{(v)}\rangle - \nabla_y\Delta\varphi^{(v)}\rangle - \gamma_u\nabla^2\Delta u^{(v)} = R_u^{(v)}, \end{aligned} \quad (61)$$

and

$$\begin{aligned} \tilde{\gamma}\Delta v^{(v)} + \alpha_t\Phi\nabla_y(-\Phi(\nabla_x\Delta u^{(v)} + \nabla_y\Delta v^{(v)})) + \gamma_t f\langle f\langle\Delta v^{(v)}\rangle - \nabla_x\Delta\varphi^{(v)}\rangle - \gamma_v\nabla^2\Delta v^{(v)} = R_v^{(v)} \end{aligned} \quad (62)$$

where $\Delta\varphi^{(v)}$, $\Delta u^{(v)}$, and $\Delta v^{(v)}$ are defined in eq (37). These equations become

$$[\tilde{\alpha} - (\gamma_t + \alpha)\nabla^2]\Delta\varphi^{(v)} + \gamma_t f\nabla_x\langle\Delta v^{(v)}\rangle - \gamma_t f\nabla_y\langle\Delta u^{(v)}\rangle = R_\varphi^{(v)}, \quad (63)$$

$$\begin{aligned} \gamma_t f\nabla_y\langle\Delta\varphi^{(v)}\rangle + (\tilde{\gamma} - \alpha_t\Phi^2\nabla_x^2 + \gamma_u\nabla^2 + \gamma_t f^2\langle\langle \rangle\rangle)\Delta u^{(v)} - \alpha_t\Phi^2\nabla_x\nabla_y\Delta v^{(v)} = R_u^{(v)}, \end{aligned} \quad (64)$$

and

$$\begin{aligned} -\gamma_t f\nabla_x\langle\Delta\varphi^{(v)}\rangle - \alpha_t\Phi^2\nabla_x\nabla_y\Delta u^{(v)} + (\tilde{\gamma} - \alpha_t\Phi^2\nabla_y^2 - \gamma_v\nabla^2 + \gamma_t f^2\langle\langle \rangle\rangle)\Delta v^{(v)} = R_v^{(v)}. \end{aligned} \quad (65)$$

Elimination of $R_\varphi^{(v)}$, $R_u^{(v)}$, and $R_v^{(v)}$ from eq (63) ~ (65) and eq (30) ~ (32) leads to simultaneous recurrence formulas

$$\begin{aligned} D_\varphi\Delta\varphi^{(v+1)} - (\gamma_t + \alpha)\left(\nabla_x^2 + \nabla_y^2 + 4\frac{1}{(2\Delta s)^2}\right)\Delta\varphi^{(v)} - \gamma_t f\nabla_y\langle\Delta u^{(v)}\rangle + \gamma_t f\nabla_x\langle\Delta v^{(v)}\rangle = 0, \end{aligned} \quad (66)$$

$$\begin{aligned} \gamma_t f\nabla_y\langle\Delta\varphi^{(v)}\rangle + D_u\Delta u^{(v+1)} + \left[-\alpha_t\Phi^2\left(\nabla_x^2 + \frac{2}{(2\Delta s)^2}\right) - \gamma_u\left(\nabla^2 + \frac{4}{(2\Delta s)^2}\right) + \gamma_t f^2\right. \\ \left.\times\left(\langle\langle \rangle\rangle - \frac{1}{4}\right)\right]\Delta u^{(v)} - \alpha_t\Phi^2\nabla_x\nabla_y\Delta v^{(v)} = 0, \end{aligned} \quad (67)$$

and

$$\begin{aligned} -\gamma_t f\nabla_x\langle\Delta\varphi^{(v)}\rangle - \alpha_t\Phi^2\nabla_x\nabla_y\Delta u^{(v)} + D_v\Delta v^{(v+1)} + \left[-\alpha_t\Phi^2\left(\nabla_y^2 + \frac{2}{(2\Delta s)^2}\right) - \gamma_v\left(\nabla^2 + \frac{4}{(2\Delta s)^2}\right) + \gamma_t f^2\left(\langle\langle \rangle\rangle - \frac{1}{4}\right)\right]\Delta v^{(v)} = 0 \end{aligned} \quad (68)$$

where the constant coefficients D_φ , D_u , and D_v are defined in eq (33) ~ (35). When considering a simple harmonic to represent $\Delta\varphi^{(v)}$, $\Delta u^{(v)}$, and $\Delta v^{(v)}$ as given in eq (38), the operators ∇_x , ∇_y , and $\langle \rangle$ are replaced by the constants $i \sin k\Delta s/\Delta s$, $i \sin h\Delta s/\Delta s$, and $\frac{1}{2}(\cos k\Delta s + \cos h\Delta s)$, respec-

tively. Using the definition of amplification matrix \mathbf{G} as defined in eq (36), one may rewrite these equations as

$$(D_\varphi\mathbf{G} + a_{11})\Delta\varphi^{(v)} + a_{12}\Delta u^{(v)} + a_{13}\Delta v^{(v)} = 0, \quad (69)$$

$$a_{21}\Delta\varphi^{(v)} + (D_u\mathbf{G} + a_{22})\Delta u^{(v)} + a_{23}\Delta v^{(v)} = 0, \quad (70)$$

and

$$a_{31}\Delta\varphi^{(v)} + a_{32}\Delta u^{(v)} + (D_v\mathbf{G} + a_{33})\Delta v^{(v)} = 0 \quad (71)$$

where

$$a_{11} = -\gamma_t + \alpha \frac{1}{(2\Delta s)^2} 4(1 - \sin^2 k\Delta s - \sin^2 h\Delta s),$$

$$a_{12} = -\gamma_t \frac{f}{2\Delta s} 2i \sin h\Delta s \cdot \frac{1}{2} (\cos k\Delta s + \cos h\Delta s),$$

$$a_{13} = -\gamma_t \frac{f}{2\Delta s} 2i \sin k\Delta s \cdot \frac{1}{2} (\cos k\Delta s + \cos h\Delta s),$$

$$a_{21} = -\gamma_t \frac{f}{2\Delta s} 2i \sin h\Delta s \cdot \frac{1}{2} (\cos k\Delta s + \cos h\Delta s),$$

$$\begin{aligned} a_{22} = -\alpha_t \frac{\Phi^2}{(2\Delta s)^2} (2 - 4 \sin^2 k\Delta s) + \gamma_t f^2 \frac{1}{4} ((\cos k\Delta s + \cos h\Delta s)^2 - 1) + \gamma_u \frac{4}{(2\Delta s)^2} (\sin^2 k\Delta s + \sin^2 h\Delta s - 1), \end{aligned}$$

$$a_{23} = \alpha_t \frac{\Phi^2}{(2\Delta s)^2} 4 \sin k\Delta s \sin h\Delta s,$$

$$a_{31} = -\gamma_t \frac{f}{2\Delta s} 2i \sin k\Delta s \cdot \frac{1}{2} (\cos k\Delta s + \cos h\Delta s),$$

$$a_{32} = \alpha_t \frac{\Phi^2}{(2\Delta s)^2} 4 \sin k\Delta s \sin h\Delta s,$$

and

$$\begin{aligned} a_{33} = -\alpha_t \frac{\Phi^2}{(2\Delta s)^2} (2 - 4 \sin^2 h\Delta s) + \gamma_t \frac{f^2}{4} ((\cos k\Delta s + \cos h\Delta s)^2 - 1). \end{aligned}$$

From eq (69) ~ (71), it is shown that the coefficients of the cubic eq (39),

$$A\mathbf{G}^3 + B\mathbf{G}^2 + C\mathbf{G} + D = 0,$$

are given as

$$A = D_\varphi D_u D_v,$$

$$B = a_{11}D_u D_v + a_{22}D_\varphi D_v + a_{33}D_\varphi D_u,$$

$$C = (a_{22}a_{33} - a_{23}a_{32})D_\varphi + (a_{33}a_{11} - a_{31}a_{13})D_u + (a_{11}a_{22} - a_{12}a_{21})D_v,$$

and

$$\begin{aligned} D = a_{11}a_{22}a_{33} + a_{12}a_{23}a_{31} + a_{13}a_{12}a_{22} - a_{31}a_{13}a_{22} - a_{32}a_{23}a_{11} - a_{21}a_{12}a_{33}. \end{aligned}$$

The roots of the cubic eq (39) for these complicated coefficients were solved by using an electronic computer.

ACKNOWLEDGMENTS

This study was sponsored partially under the National Science Foundation Research Grant GF-291 provided under the United States-Japan Cooperative Science Program and supported by the Environmental Science Services Administration under ESSA Research Grants E22-17-69(G) and E19-69(G).

Acknowledgment is made to the National Center for Atmospheric Research, sponsored by the National Science Foundation, for use of its Control Data 6600 computer and also the Merrick Computer Center of The University of Oklahoma for use of the IBM 360/40 computer.

The author wishes to express his appreciation to Dr. J. M. Lewis of The University of Oklahoma and Mr. Robert C. Sheets of the National Hurricane Research Laboratory for their valuable assistance given in the course of this study and also to Mrs. Keven Amrein for her assistance in preparing the manuscript.

REFERENCES

- Bolin, Bert, "Numerical Forecasting With the Barotropic Model," *Tellus*, Vol. 7, No. 1, Feb. 1955, pp. 27-49.
- Charney, Jule G., "The Use of the Primitive Equations of Motion in Numerical Prediction," *Tellus*, Vol. 7, No. 1, Feb. 1955, pp. 22-26.
- Courant, R., and Hilbert, D., *Methods of Mathematical Physics*, Vol. 1, Interscience Publishers, Inc., New York, 1953, 561 pp.
- Courant, R., and Hilbert, D., *Methods of Mathematical Physics*, Vol. 2, Interscience Publishers, Inc., New York, 1962, 830 pp.
- Cressman, George P., "An Operational Objective Analysis System," *Monthly Weather Review*, Vol. 87, No. 10, Oct. 1959, pp. 367-374.
- Gandin, Lev S., *Objective Analysis of Meteorological Fields (Ob'ektivnyĭ analiz meteorologicheskikh polei*, 1963), Israel Program for Scientific Translations, Jerusalem, 1965, 242 pp.
- Hinkelmann, Karl, "Ein Numerisches Experiment mit den Primitive Gleichungen" (A Numerical Experiment With the Primitive Equations), *The Atmosphere and the Sea in Motion*, Rockefeller Institute Press, New York, 1959, pp. 486-500.
- Miyakoda, K., and Moyer, R. W., "A Method of Initialization for Dynamical Weather Forecasting," *Tellus*, Vol. 20, No. 1, 1968, pp. 115-128.
- Nitta, Takashi, and Hovermale, John B., "A Technique of Objective Analysis and Initialization for the Primitive Forecast Equations," *Monthly Weather Review*, Vol. 97, No. 9, Sept. 1969, pp. 652-658.
- Phillips, Norman A., "On the Problem of Initial Data for the Primitive Equations," *Tellus*, Vol. 12, No. 2, May 1960, pp. 121-126.
- Sasaki, Yoshikazu, "An Objective Analysis Based on the Variational Method," *Journal of the Meteorological Society of Japan*, Ser. 2, Vol. 36, No. 3, June 1958, pp. 77-88.
- Sasaki, Yoshikazu, "Numerical Variational Method of Analysis and Prediction," *Proceedings of the WMO/IUGG Symposium on Numerical Weather Prediction, Tokyo, Japan, November 26-December 4, 1968*, Japan Meteorological Agency, Tokyo, Mar. 1969a, pp. VII-25-VII-33.
- Sasaki, Yoshikazu, "Proposed Inclusion of Time Variation Terms, Observational and Theoretical, in Numerical Variational Objective Analysis," *Journal of the Meteorological Society of Japan*, Vol. 47, No. 2, Apr. 1969b, pp. 115-124.
- Sasaki, Yoshikazu, "Some Basic Formalisms in Numerical Variational Analysis," *Monthly Weather Review*, Vol. 98, No. 12, Dec. 1970a, pp. 875-883.
- Sasaki, Yoshikazu, "Numerical Variational Analysis With Weak Constraint and Application to Surface Analysis of Severe Storm Gust," *Monthly Weather Review*, Vol. 98, No. 12, Dec. 1970b, pp. 900-912.
- Sasaki, Yoshikazu and Lewis, J. M., "Numerical Variational Objective Analysis of the Planetary Boundary Layer in Conjunction With Squall Line Formation," *Journal of the Meteorological Society of Japan*, Ser. 2, Vol. 48, No. 5, Oct. 1970, pp. 381-399.
- Sheets, Robert C., "The Three-Dimensional Large Scale Structure of Hurricane 'Dora' (1964)," *Report ARL-1470-1*, Grant NSF GF-172, Atmospheric Research Laboratory, The University of Oklahoma, Norman, Oct. 1965, 30 pp.
- Todd, J., Editor, *A Survey of Numerical Analysis*, McGraw-Hill Book Co., Inc., New York 1962, 589 pp.

[Received March 6, 1970; revised April 23, 1970]